



HAL
open science

Structure of the Tectonic Front of the Western Alps: Control of Fluid Pressure and Halite Occurrence on the Decollement Processes

Eric Deville

► **To cite this version:**

Eric Deville. Structure of the Tectonic Front of the Western Alps: Control of Fluid Pressure and Halite Occurrence on the Decollement Processes. *Tectonics*, 2021, 40 (4), pp.e2020TC006591. 10.1029/2020tc006591 . hal-03248807

HAL Id: hal-03248807

<https://ifp.hal.science/hal-03248807>

Submitted on 3 Jun 2021

HAL is a multi-disciplinary open access archive for the deposit and dissemination of scientific research documents, whether they are published or not. The documents may come from teaching and research institutions in France or abroad, or from public or private research centers.

L'archive ouverte pluridisciplinaire **HAL**, est destinée au dépôt et à la diffusion de documents scientifiques de niveau recherche, publiés ou non, émanant des établissements d'enseignement et de recherche français ou étrangers, des laboratoires publics ou privés.

Structure of the tectonic front of the Western Alps: Control of fluid pressure and halite occurrence on the decollement processes

E. Deville¹

¹IFP Energies nouvelles, IFP School, 1-4, av. de Bois-Préau, 92 506 Rueil-Malmaison, France

Corresponding author: Eric Deville (eric.deville@ifpen.fr)

<https://orcid.org/0000-0002-5908-5796>

Key Points:

- The structure of the front of the Alps is controlled by the occurrence of halite and fluid pressure condition
- Shift of decollement level induces tectonic subtraction or duplication
- Change in the thickness of the sediments involved in the tectonic wedge induces differential propagation of the tectonic front

This article has been accepted for publication and undergone full peer review but has not been through the copyediting, typesetting, pagination and proofreading process, which may lead to differences between this version and the [Version of Record](#). Please cite this article as [doi: 10.1029/2020TC006591](https://doi.org/10.1029/2020TC006591).

This article is protected by copyright. All rights reserved.

Abstract This study focuses on the respective role of (1) the occurrence and the nature of evaporitic layers and (2) the fluid pressure conditions on the decollement processes and the structure of the foreland fold and thrust belt of the Western Alps. The decollement in the Jura Mountains is predominantly localized in halite-bearing layers. Anhydrite-bearing units which are not associated to halite are not hosting major decollement. The shift of decollement level between Mid-Triassic halite unit and Upper Triassic halite unit has induced local tectonic subtractions and, elsewhere, tectonic duplications at depth. Available fluid pressure measurements show that fluids are not overpressured in the Jura. Even below the salt decollement, they remain in hydrostatic conditions. South of the Jura, the absence of halite is correlated with no efficient role of the Triassic layers in terms of decollement. The available pressure measurements show that the decollement is associated with high overpressure. Because of the low friction of halite, the Jura thrust wedge shows a narrow angle (3 to 4°). The relatively high friction behavior of the decollement south of the Jura is responsible for stacks of tectonic units associated with a relatively wide angle of the tectonic wedge (12 to 13°). The structural change between the Chartreuse and Vercors massifs is not controlled by the properties of the decollement but by the change of thickness of the sedimentary pile involved in the tectonic wedge. The change of thickness is controlled by paleogeographic heritage during Jurassic and Cretaceous times.

Key words: Western Alps, tectonic front, fold-and-thrust belt, pressure, halite, decollement.

1. Introduction

Despite a long history of geological studies, the deep structure of the tectonic front of the Western Alps (Figs. 1, 2) remains poorly known, mainly because of the lack of available published seismic reflection studies and because of only few wells available providing deep calibration. The published data which offers a seismic information along a full transect across the foreland fold-and-thrust belt of the western Alps (including Jura Mountains) was provided by the research program ECORS-ALP of deep seismic acquisition (Guellec et al., 1990a and b; Mugnier et al., 1990; Bergerat et al., 1990) and by the processing of some industrial seismic lines that gave information on a full transect of the western Alps front along the Chambéry transect (Deville and Chauvière, 2000). Also, few seismic lines have been punctually published in the Molasse Basin (Charollais and Jamet, 1990; Wildi and Huggenberger, 1993; Gorin et al., 1993; Deville et al., 1994a and b; Beck et al., 1998) and in the inner part of the Jura Mountains (Sommaruga, 1997; 1999; 2011; Sommaruga et al., 2012, 2017; Rime et al., 2019). Due to the lack of constraining subsurface data, several fundamental structural problems remain still unsolved. Notably, the former published structural cross-sections show very different interpretations concerning the structure of the basement and its possible involvement in thrust tectonics. Some hypotheses suppose a significant overthrusting (several kilometers) involving the basement under the Subalpine chains (Ziegler, 1994; Menard and Mugnier, 1986; Thouvenot and Menard, 1990). Most of the authors suppose that the basement is not or only weakly involved under the sole thrust of the detached sedimentary cover, except locally in the form of tectonic inversion of Carboniferous-Permian basins (Guellec et al., 1990a; Pfiffner et al., 1997, 2016). Another, recumbent matter of discussion concerns the exact location and the nature of the decollement which has controlled the structuration of the front of the Western Alps. In the Jura Mountains, since Buxtorf (1907, 1916), it is generally considered that the decollement is hosted within Triassic salt mainly of late Triassic age (Keuper), and also in Mid-Triassic salt layers (Muschelkalk) in north-eastern Jura (Jordan and Nuesch, 1989a; Jordan et al., 1990; Jordan, 1992; Philippe et al., 1996; Sommaruga, 2017; Fig. 2). Thrust fault throws and global tectonic shortening are also common subjects of debate. Some authors claimed that the thrust throws of the Alpine front are very moderate (Gidon, 1981; 1988), whereas other authors considered that several tens of kilometers of tectonic shortening have been recorded within the foreland fold-and-thrust belt (FTB) of the Western Alps (Laubscher, 1972; Doudoux et al., 1982; Guellec et al., 1990a; Mugnier et al., 1990; Philippe et al., 1996; Mascle et al., 1996; Pfiffner et al., 1997;

Sommaruga, 1999; Deville and Sassi, 2006). The reactivation processes of the extension structures of the rift system within the Alpine front is a subject which has been addressed only punctually (Deville et al., 1994b; Philippe et al., 1996; Deville and Sassi, 2006). Also, the timing of the deformation remains a constant topic of discussion all along the Alpine tectonic front facing the European foreland (see Granado et al., 2016).

In order to provide a better knowledge of the structure, the tectonic processes and the timing of deformation which have affected the Western Alps foreland fold-and-thrust belt, a selection of available industrial seismic data has been reprocessed and reinterpreted integrating results of well data in Central Jura and in the Subalpine chains. Beyond simple structural descriptions, the purpose of this study focusses on the role of the nature and the thickness of the sediments involved in the tectonic wedge and to identifying the nature and the position of the decollement levels and their role in the global deformation of the thrust system. We notably analyzed the information provided by several wells cross-cutting the decollement levels, especially the presence and the nature of evaporitic levels and the role of fluid pressure at the decollement level and below.

2. Geodynamic framework of the Western Alps tectonic front

As initially proposed by Buxtorf (1907) who first introduced the notion of decollement, the deformation of the thrust wedge of the Jura Mountains, the Savoy and Swiss Molasse basin and the Subalpine chains is resulting from a decollement located within the sedimentary formations and rooted within the Alps, the whole system forming the tectonic front the Western Alps. Following Buxtorf's hypothesis, it is commonly admitted that the thrust wedge corresponds to deformed Mesozoic and Cenozoic sedimentary formations incorporated within a classical foreland FTB which developed during Tertiary late Alpine collision stages at the front of the tectonic thrusting of the Pre-Triassic basement of the External Crystalline Massifs (ECM) of the Western Alps (Mont Blanc-Aiguilles Rouges-Belledonne massifs; Fig. 1) (Laubscher, 1961, 1981; Doudoux et al., 1982; Guellec et al., 1990a and b; Mugnier et al., 1990; Butler, 1992; Deville et al., 1994a and b; Deville and Sassi, 2006; Bellahsen et al., 2014 and many others). The Western part of the tectonic front of the Alpine collisional belt propagated during Neogene times within the European Alpine foreland which had been already deformed at that time by the former extensional structures related to (1) the development of the Mesozoic north Tethyan passive margin, and (2) the development of the West European rift system during Late Eocene to Early Miocene times (Laubscher, 1972;

Philippe et al., 1996; Madritsch et al., 2008; Malz et al., 2019; Fig. 1). The Alpine orogenic front accommodates, within the sedimentary cover of the Alpine foreland, the last frontal few tens of kilometers of the several hundred kilometers of NW-directed shortening recorded in the lithospheric wedge of the Western Alps during Tertiary times with the involvement of wide mantle bodies (Thouvenot et al., 1990; Tardy et al., 1990; Deville, 2015; CII and CIP in Fig. 1B). As a main result of the ECORS-CROP French-Italian scientific program during the 80's, it is now commonly admitted that the tectonic involvement of the European continental crust in a major thrusting structure is responsible for the uplift of the External Crystalline Massifs (ECM: Mont-Blanc-Aiguilles rouges-Belledonne massifs) and for the deformation of the sediments within the foreland associated with a tectonic shortening of 30 to 35 km (Tardy et al., 1990; Guellec et al., 1990; Mugnier et al., 1990; Fig. 1B). The thrusting of the ECM is very probably rooted within the mantle as suggested by the results of wide angle reflection experiments (Thouvenot et al., 1990; Fig. 1B). This is also the case for the Penninic tectonic front which separates the outer zones from the inner zones of the Alps in which HP-LT Tertiary metamorphic rocks are found (Tardy et al., 1990; Fig. 1B). The whole shortening related to the collision between the Europe-Asia tectonic plate and the Adria block is responsible the development of a lithospheric root at depth which is longer than 300 km below the Po valley (Lippitsch et al., 2003; Hua et al., 2017; Fig. 1B). A relatively moderate deformation of the European crust NW of the ECM is also responsible for inversion processes of a Permian-Carboniferous basin the basement and for a probably newly-formed tectonic layering of the lower continental crust visible on the ECORS deep seismic data (Guellec et al., 1990a; Fig. 1B).

In the study area of the Alpine foreland, above the Pre-Triassic basement, after periods of emersion during the Triassic associated locally with the deposition of evaporites, marine conditions prevailed during Mesozoic times, and several paleogeographic domains developed along NE-SW trending areas (Fig. 1). (1) The Jurassian platform (Jura, Molasse Basin and Valence Basin) is characterized by thick Jurassic-Cretaceous platform carbonates. In the western part of this domain, Tertiary erosion has removed the Cretaceous formations prior to thrust tectonics, whereas these deposits are still preserved under a platform facies in the eastern area. (2) The intermediate Pre-Subalpine domain (including the outer parts of the Bauges, Chartreuse and Vercors massifs; Charollais et al., 1996). This intermediate domain forms the transition zone (slope) between the platform and the Subalpine basin. It corresponds to the northeastern prolongation of the Ardèche margin which includes a fault system related to the Lias-Dogger Tethyan rifting (Masclé et al., 1996; Bonijoly et al., 1996; Sanchis and

Seranne, 2000; de Graciansky et al., 2011; Fig. 2). (3) The Subalpine basin (Bornes massif and the inner parts of the Bauges, Chartreuse and Vercors massifs) that corresponds to a thick sedimentary area including the northwestern-most Mesozoic tilted-blocks of the Late Jurassic-Cretaceous north-Tethyan passive margin. During Tertiary times, the paleogeography changed in relation to the West-European rift development (Ziegler et al., 1994) and to Alpine deformation. During Eocene to Aquitanian times, the West-European rift system developed in the western area shown in Fig. 2, and erosion processes occurred due to the uplift of the shoulders of the rift system (Bresse, Valence and south-east basin of France), whereas clastic formations were deposited in the eastern part, related to the lithospheric flexure associated with tectonic loading in the inner zones of the Alps during the early stages of collision between Adria and the Eurasian plate. Then, the region was progressively involved in the Alpine thrust tectonics from the Subalpine domain to the Jura. The deformation of the FTB of the Western Alps started in the inner Subalpine chains (Bornes and Bauges) in Late Oligocene-Early Miocene times by the tectonic emplacement of the Prealps nappe (Fig. 2). It is generally admitted that the whole Alpine frontal thrust wedge has been mostly active during Miocene times. During this period the whole tectonic wedge has been detached above the basement (Laubscher, 1972; Guellec *et al.*, 1990a; Burkhard and Sommaruga, 1998; Deville et al., 1994a; Philippe *et al.*, 1996; Mascle et al., 1996; Affolter and Gratier, 2004; Deville and Sassi, 2006). The deformation of the Subalpine massifs was characterized by the stacking of thrust sheets and the development of duplexes as it has been evidenced by drilling in the Bornes massif (Charollais and Jamet, 1990, Guellec *et al.*, 1990a; Deville and Sassi, 2006). Thrust tectonics involved the Savoy Molasse Basin and the inner Jura at least since the Burdigalian and syntectonic Burdigalian to Serravalian sedimentation occurred within the piggy-back basins developed between thrust anticlines of the Molasse Basin (Deville et al., 1994a; Beck et al., 1998). It has been shown that the front of the Jura wedge is thrust over Uppermost Miocene (Messinian) sediments for several kilometers in the Bresse Basin (Michel et al., 1953; Chauve et al., 1988). This timing of deformation is compatible with radiogenic U-Pb dating of syntectonic veins in the decollement zone (Looser et al., 2021). However, the complete timing of the propagation of the deformation within the Alpine thrust system is not fully constrained, as well as the late activation or re-activation of most of the inner thrust structure of the Alpine front. Notably, it has been shown that the last period of activation of the subalpine front in the Bauges massif is late and out-of-sequence as the front of the Bauges massif is thrust over Langhian-Serralian sediments (probable late Miocene to Pliocene re-activation; Deville et al., 1994a; Deville and Chauvière, 2000). Similar period of tectonic

activity at the Alpine front has been proposed by von Hagke et al. (2012) and Mock et al. (2020) in Switzerland.

3. Material and methods

A selection of seismic profiles and available drilling results has been used to address the structural problems mentioned above. Geophysical data presented in this study are based on the processing of available industrial seismic data in the Jura area and on non-exclusive IFP-CGG acquired in the Chartreuse and Vercors area (FSH 82SE and Chartreuse-Vercors 91 surveys). Some data has been partly published in Deville et al., 1994b and Deville, 2015. We present also an interpretation of a composite line at the French-Swiss border in the Jura area which has been presented in Anna Sommaruga's PhD (un-interpreted section of plate 8A in Sommaruga, 1997). The geophysical data presented in this study have been chosen where well calibrations are available along the seismic lines in order to be able to propose reliable structural interpretation and depth conversion for a better definition of the structure of the tectonic wedge, notably simply the geometry of the taper of the thrust wedge. Seismic data to well data were tied using check-shots when available or with synthetic seismograms made from sonic and density electric logs (see supplementary material). These data were used for time to depth conversion to draw geological cross-sections. As the discussion of this paper focusses on decollement processes which occur preferentially in salt or clay-rich sediments, detailed wells results deduced from cuttings have been presented in figure 4 and available electric logs have also been used to characterize the rocks specifically at and around the decollement level. This has been done notably to identify the location and the nature of salt units (see figures 4 and 6 where available gammay-ray logs are shown). Pressure measurements issued from available drilling reports have been compiled on a selection of wells (Table 1).

4. Interpretation of drilling and seismic data

Drilling results have demonstrated that the general structure of the Jura corresponds to a thin tectonic wedge in the outer part (NW) and this wedge thickens progressively toward the inner part (SE). This is well illustrated in the seismic data on which the tectonic wedge appears relatively thin in the outer Jura (several hundred meters; Fig. 3B) and thicker in the inner Jura (> 2 km; Fig. 3C, D). The seismic data does not show any evidence for the involvement of the

Accepted Article

basement in the study area. The frontal part of the Jura Mountains is characterized by mixed compressional structures and passively transported extension structure inherited from the rifting phase during late Eocene-Oligocene-Aquitania times (Michel et al. 1953; Philippe et al., 1996). In the central Jura (Fig. 3A), two wells have demonstrated that, at depth, around the decollement level, the Upper Triassic is duplicated in the Valempoulières area which corresponds to a small gas field (Philippe et al., 1996; Fig. 3B), whereas it is missing in the CHA-1 well (Fig. 3C). Drilling results are compatible with seismic data which indeed show the duplication of the Upper Triassic where the Upper Triassic sediments are overthrust by a complete series from the Lower Keuper salt to the Jurassic. The overthrust Upper Triassic forms a thin unit which is clearly visible on the seismic data above the decollement (Fig. 3B). Note also that disharmonic folding are common in Liassic, Mid-Jurassic and Lower Cretaceous formations and that secondary decollements are known in the Jura Mountains, notably in the inner Jura (high chain), at the transition between the Jurassic and the Cretaceous sequences. This transition corresponds to an emersion period known in Western Europe (Purbeck formation), in which marl, shale and evaporite are low resistance layers prone to favor secondary decollement. Indeed, as demonstrated by drilling data, the inner part of the Jura (high chain) is characterized by spectacular overthrusting in the Risoux area which is characterized by the duplication of the Jurassic series (Winnock, 1961; Aubert, 1971; Rigassi, 1977; Philippe et al., 1996; Sommaruga, 1997; Fig. 3E).

South of the Jura, there is no available drilling data within the Chartreuse massif, only wells located in the foreland west of the Chartreuse tectonic front which provide a calibration of the seismic reflectors which are well visible in the foreland (section *I-I'*, Fig. 5). These reflectors can be followed in the seismic data toward the tectonic front. Notably, a set of about 0.1 sTWT thick reflectors appears in the western part of the section *I-I'* of figure 5 in the window 1.2 to 1.5 sTWT. These reflectors can be tied using well data and seismic data (Fig. 6A). They can be followed from the PA-1 well (in the autochthonous foreland) all along the seismic section *I-I'* of figure 5. The well calibration has shown that these reflectors correspond to Triassic formations. This demonstrates that the Triassic is not involved in thrust tectonics along the Chartreuse massif. The basal decollement in the Chartreuse massif is thus located above the Triassic, very probably within the base of the Jurassic series (Lias and/or Dogger). Within the tectonic front of the Chartreuse massif, the integration of surface data and seismic data is compatible with the stacking of several tectonic units involving formations from the Jurassic to the Miocene as shown in Deville and Sassi (2006). The thrust faults within the Chartreuse massif are secant on Lower Miocene sediments but the thrust front of the

Chartreuse massif is blind as it is covered by a syn-tectonic fan of Mid- to Late Miocene age (Fig. 5A). The timing of the late throws of the inner thrust in Chartreuse is not known precisely but the thrust of eastern Chartreuse is connected to the thrust of the front of the Bauges massif which is known to be still active at least after the Serravalian (Deville et al., 1994a; Deville and Chauvière, 2000; see above in the geological framework).

The seismic line shot in the Isere valley between the Chartreuse and the Vercors massifs has shown that the Mesozoic series is tectonically duplicated at the structural front of this area (section *II-II'*, Fig. 5B). Note that the structural image of the structural front is hampered in this area due to glacial deep erosion during Quaternary glaciations and subsequent thick fluvial-lacustrine sedimentary deposition (> 0.5 sTWT in the seismic data). West of the tectonic front, the tectonic thickening of the Mesozoic series is well characterized on the seismic data and it is also associated to a stratigraphic thickening of the sedimentary series (transition from the platform domain to the Pre-Subalpine and Subalpine domains). The stratigraphic thickening is associated with a seismic facies change characterized by a loss of the seismic layering between the Jurassic platform and the Jurassic-Cretaceous formations of the Subalpine basin. The stratigraphic thickening is controlled by the activity of normal faults which were active during Mesozoic times. A moderate inversion process probably occurred close to the Mesozoic fault system during Alpine compression (Polienas fault, section *II-II'*, Fig. 5B). Below the reflector assigned to the Triassic, the Pre-Triassic basement does not show continuous reflectors except in the central area where some layered reflectors would probably correspond to sedimentary formations (probable Carboniferous-Permian basin).

The structure of the Vercors tectonic front is organized as an en-echelons fault and fold system (*III-III'*, Fig. 5C). The seismic data tied to well results which are available in the Vercors area shows that the Late-Eocene to Aquitanian extension structures of the Valence Basin (west European rift system) have been deformed by the Miocene to recent time processes of thrust tectonics related to the propagation of the Alpine front. Pre-existing Eocene to Aquitanian normal faults have been passively displaced above the basal decollement of the Vercors thrust system and the related grabens or half-grabens are today incorporated within the core of ramp anticlines forming transported inversion structures (Deville et al., 1994b; section *III-III'*, Fig. 5C). Such structures are similar in the Saint-Lattier and the Saint-Nazaire anticlines which suggest that thrust faults have been initiated along the lower parts of the pre-existing normal faults. Well data have shown that the decollement is localized within Lias-Dogger formations (Fig. 6C). As it is the case for the Chartreuse area (see above), the Triassic is not involved in thrust tectonics in the Vercors massif. Notably, the

anhydrite layers which are present within the Triassic are not hosting the decollement and they do not show evidence of important deformation (Fig. 5 and 6). The thrust faults within the Vercors massif are secant on Lower Miocene sediments but the frontal thrusts in the Saint-Lattier, in Saint-Nazaire and in Pont-en-Royans areas are blind as they are covered by syn-tectonic sediments (piggy-back basin) of Mid- to Late Miocene age (section *III-III'*, Fig. 5C). The timing of the late throws of the inner thrusts in Vercors is not known.

5. Discussion

Decollement processes in evaporites: halite versus anhydrite

The structural study of the geophysical data and well data (final drilling reports supported by cutting and electric logs analysis) has shown that the basal decollement of the thrust wedge of the Jura Mountains is located in halite-bearing units (Fig. 4). Indeed, the decollement in the Jura Mountains is localized within two distinct evaporite units which contain halite: (1) the Early Keuper (Carnian) and (2) the Mid-Muschelkalk (Anisian) halite-bearing units (Fig. 4). In previously published works or during this study, nowhere it has been possible to characterize decollement processes in the Jura Mountains in anhydrite which is not associated to halite. The most intense deformation processes (ductile shearing) which have been characterized in anhydrite of the Jura were found in anhydrite layers interbedded with dolomite layers located directly above thick layers of halite (Jordan and Nuesch, 1989a; Jordan et al., 1990; Jordan, 1992). Massive anhydrite-bearing units which are not associated to halite are not affected by long distance decollement tectonics. Indeed, Notably, the thick Late Keuper (Norian) anhydrite-claystone unit has shown no evidence for decollement activity: It has been passively transported and folded without evidence for significant detachment processes or even significant change of thickness like other non-evaporite layers (Fig. 4A and B). Similarly, the anhydrite layers which are locally present in Triassic formations south of the Jura Mountains (in the Valence basin or in the front of the Subalpine chains) show no evidence for decollement (Fig. 5 and 6). These observations are consistent with the fact that mechanical experiments have demonstrated that anhydrite-halite viscosity ratio is very high (>8) especially at temperatures lower than 120°C (Ross and Bauer, 1992; Jordan, 1992), which is the case for temperature measurements made while drilling in the study area and which was very probably the case during tectonic shortening in the Jura. As such, halite is indeed much more favorable for decollement processes than anhydrite. In the

study area, as well as in other parts of the Jura (see notably Jordan and Nuesch, 1989b), halite layers being closely interbedded with shale, the decollement is localized along planar zones of deformation within the halite-bearing units. As deduced from the drilling results, these zones of deformation are probably thinner than 20 to 30 m. This is in agreement with the analysis of the seismic data, where the thickness of these deformation zones appears to be less than one or two seismic phases. The halite-bearing units do not show evidence for massive processes of viscous deformation like diapirism (no piercing body of salt, only salt pillow and salt-cored anticlines). The area where halite has been mobilized the most corresponds to the salt pillow around the TLN-1 and LAV-1 wells (Philippe et al., 1996; Sommaruga, 1997; Fig. 3 and 4). No piercing salt diapir is known in the Jura Mountains.

Decollement processes in shale and marly shale: active fluids and passive fluids

The basal friction at the base of FTB is controlling the structures generated within the tectonic wedges (King-Hubbert, 1951). The mechanical equilibrium of a subaerial thrust system is accomplished when the sum of the forces forming the load of the wedge and the shear strength at the base of the wedge compensate the tectonic force. The basal decollement of a tectonic wedge must be weaker than the material within the wedge in order for sliding to occur at the base. The simplified critical taper equation which describes the geometry of a thin tectonic wedge can be written as (derived from Dahlen, 1990):

$$\alpha + \beta = \frac{(1 - \rho_f / \rho)\beta + \mu_b(1 - \lambda_b)}{(1 - \rho_f / \rho) + W}$$

with α = wedge taper (in radians), β = dip of the decollement (in radians), ρ and ρ_f are the densities of the rocks and fluids, respectively, within the wedge, μ_b = coefficient of friction of the basal decollement, W = internal strength of the wedge material, $\lambda_b = P_{fb} / \sigma_v$ with P_{fb} = fluid pressure at the decollement level, σ_v = vertical stress.

When decollements are located in ductile layers, fluids do not have a specific role for the activity of the decollements except if the dehydration of gypsum into anhydrite during burial or tectonic processes induces overpressure. On the other hand, in absence of evaporites, the fluids play a very crucial role (Hubbert and Rubey, 1959; Chapple, 1978; Byerlee, 1978;

Davis *et al.*, 1983; Dahlen *et al.*, 1984; Dahlen, 1990; Cobbold *et al.*, 2000). In the case study, in a first approximation, the internal strength of the wedge can be considered as globally equivalent all along the study area but drastic changes occur concerning the shear strength at the base of the wedge due to very low coefficient of friction of halite-bearing units when present and to fluid pressure condition when halite is absent. As mentioned above, the decollement of the Alpine front, in the Jura area, is localized within the Triassic halite-bearing units (mainly in the Early Keuper and locally in the Mid-Muschelkalk; Fig. 4).

μ_b of halite is classically considered to be very low and wedges above thick salt decollement are considered to have $\alpha+\beta$ values of about 1° (Davis *et al.*, 1983; Dahlen, 1990). This is the case for instance of the Angolan gravity system (Hudec and Jackson, 2004), of the Nova Scotia gravity system (Deptuck, 2009), or else the Gulf of Mexico gravity system (Peel *et al.*, 1995; Trudgill *et al.*, 1999). Similar angle is observed in the Zagros FTB which is also detached above thick salt layers (Verges *et al.*, 2011). In the case studied here, the presence of clay-bearing material interbedded with halite (as confirmed notably with gamma-ray results; Fig. 4) tends obviously to increase μ_b and the shape of the wedge is actually tending toward an angle between 3 and 4° in the Jura Mountains.

In absence of halite, μ_b remains high and it is the fluid pressure which favors low friction at the decollement as λ_b increases. In the case studied here, $\alpha+\beta$ is comprised between 12 and 13° in Chartreuse and Vercors (Fig. 9), which is characteristic of high basal friction wedges detached in overpressured shale-rich layers (Davis *et al.*, 1983; see below).

Fluid pressure condition in aerial systems can be simply characterized by the following ratio,

$$R = \frac{P_f}{\rho_{ws} g (z-h)}$$

With P_f = fluid pressure at a depth z below soil surface, ρ_{ws} fluid density within the sediments, g gravitational acceleration, and h the depth of the top of the hydrosphere below surface. If $R = 1$ fluids can be regarded as being in hydrostatic conditions, if $R > 1$ fluids are in overpressure conditions. The excess of pressure versus hydrostatic condition is given by $P_f - \rho_{ws} g z$. Because all these parameters can be measured, the R ratio is providing a better estimate of the fluid pressure conditions than $\lambda_b = P_{fb}/\sigma_v$ because σ_v cannot be easily measured directly (just estimated).

In the Jura thrust wedge, pressure measurements have revealed no fluid overpressure conditions but, on the contrary, there are conditions of underpressure when referring to depth below surface (Fig. 7A). The fluid pressure regime in the formations located below the basal halite-bearing decollement and those located above are totally disconnected (Fig. 7; Table 1). In the geological formations located below the decollement, in the halite-bearing units, *i.e.* in the Buntsandstein (Early Triassic) and the Muschelkalk (Mid-Triassic), pressure measurements are actually compatible with hydrostatic condition of fluid pressure (R ratio ~1) with a linear fluid pressure gradient *versus* depth of 10.6 KPa/m and an equilibrium level with atmosphere at 250 m of elevation above sea level, which is equivalent to the average altitude of the Jura tectonic front (Fig. 8). This corresponds to normal hydrostatic condition of salted water with an average density of 1.07 g/cm³, which is consistent with the available salinity measurements of formation water below the Jura decollement which exhibit values reaching 304 g/l with an average value of 120 g/l (see table S1 in supplementary material). Obviously, there are therefore connections between pre-salt Triassic aquifers and atmosphere. Above the halite-bearing units, the pressures are in equilibrium at variable levels (depending on local hydrodynamic conditions) without corresponding to overpressure (Fig. 7). This compartmentalization between aquifers located below and above the salt decollement is locally responsible for inverse pressure gradients, notably on the CHA-1 well (Fig. 7). As, overall, no overpressure can be characterized in the Jura area, fluids can be regarded as passive and ineffective for the activity of the basal decollement.

In the southern part of the study area, in the Valence basin and in the front of the Subalpine chains, overpressure conditions have been characterized below a fluid retention depth of 1000 m within the Mesozoic series (Fig. 7). Possibly the overpressure generation was associated with hydrocarbon generation which occurred at the same time as thrust tectonics in the front of the Chartreuse and Vercors massifs (Deville and Sassi, 2006). The overpressure is high in the Vercors tectonic front (*cf.* well SL-2). In this case, fluids clearly play a crucial role for the activity of the decollement. Indeed, south of the Jura Mountains, the basal decollement of the Subalpine chains is not localized within evaporitic sedimentary systems but in shale and marly sediments of Lias-Dogger age (Fig. 5), precisely in the levels where the highest pressures were measured (Fig. 6). Therefore, we consider that, in this case, the decollement is controlled by high overpressure in clay-rich sediments instead of being controlled by the presence of halite like in the Jura.

Control of heritage on the nature of the decollement

Data analysis suggests a major role played by the distribution and nature of the evaporites related to the Triassic paleogeographic heritage in the structure of the orogenic front and also by the role of fluids during deformation. Indeed, it is possible to characterize different deformation processes controlled by the initial paleogeography. For the same global shortening recorded within the Alpine front (roughly corresponding to the shortening related to the crustal thrust of the ECM; *i.e.* between 30 and 35 km; see above), very different deformation processes occurred depending of the different paleogeographic areas of the foreland. The role of the inheritance related to the nature of the decollement levels has been suggested several times (Deville et al., 1994b, 2015; Philippe et al., 1996). It is possible to highlight the role of the coefficient of basal friction (μ_b) of the detachment level which is particularly well illustrated if we compare, for example, the structure of the Jura (domain with low basal friction coefficient linked to the presence of Triassic halite) and the structure of the external Chartreuse (area with high basal friction without the presence of Triassic halite) (Fig. 2). Indeed, in these two areas, the Alpine deformation affected very similar sedimentary series, except the nature of the decollement level (mainly Jurassic platform series) and, however, they are showing very different structural features (Fig. 8), notably concerning the general shape of the tectonic wedges. The Valence Basin and Subalpine chains have been affected by a strong late uplift which was characterized in the eastern Valence Basin by the fact that marine Miocene sediments have been uplifted at least up to a present-day elevation of 952 m. These sediments are preserved on top of the present-day erosional surface which includes creeks and valleys which have locally an elevation lower than 190 m and line of Fig. 5B shows that locally erosion incised down to more than 0.5 sTWT below surface (so several hundred of meters below surface, meaning actually locally below sea level). The uplift is probably related to important erosion processes which affected the core of the Alps during Late Miocene to Quaternary times (notably associated to Messinian sea level drop in the Mediterranean Sea and to Quaternary glacial period) and which is responsible for important isostatic re-equilibrium processes at lithospheric scale due to unloading related to erosion. Considering α the average slope of the topography of the tectonic wedge and β the slope of the decollement (see above), α was lower and β was higher during thrust tectonics because of the tilt associated with the uplift. Therefore, these angles cannot be used directly as geomechanical parameters to constraint the friction at the base of the wedge. However, it can

be considered that the sum $\alpha+\beta$ forming the global angle of the wedge (taper) was similar during thrust tectonics or slightly higher because of erosion after thrust tectonics.

If we simply consider today's angle of the tectonic wedge of the Jura massif, it corresponds to a thin tectonic prism where $\alpha+\beta$ is comprised between 3 and 4° (Davis and Engeler, 1985; Mugnier and Vialon, 1986; Philippe et al., 1996). This low angle corresponds to the fact that the very low basal friction of the halite decollement in the Jura made possible to propagate the stresses to the Jura tectonic front very far across the foreland forming a very thin almost ideal Mohr-Coulomb prism with low friction at the base and high strength of the wedge (Philippe et al., 1996; van Hagke et al., 2014). Wedges whose $\alpha+\beta$ value is lower than 4° are indeed characteristic of decollement in halite layers like deltaic gravity system detached above salt layer (see above).

The Chartreuse massif exhibits a characteristic stack of thrust sheets ('imbricated fan') constituting a thick wedge with an angle $\alpha+\beta$ between 12 and 13° and with a very strong internal shortening (Fig. 8), of which the corollary is a moderate westward propagation of the Alpine front with respect to the ECM indenter (<35 km) compared to the Jura > 120 km or the Vercors (> 50km; Fig. 2). This is linked to the fact that the decollement is no longer located in halite layers and, therefore, the friction at the base of the prism is higher than in the Jura where the base of the prism tends to be viscous. This angle was probably even higher at the time of the thrust propagation (Miocene) because parts of the tectonic wedge have been eroded since that time.

The Vercors massif is characterized by wedge geometry with an angle $\alpha+\beta$ between 12 and 13° very similar to the Chartreuse wedge angle (Fig. 8B). This suggests similar basal friction conditions in these two areas (the lithology inside the wedge being very similar in these two massifs).

Tapers higher than 4° are common in the fronts of accretionary prisms, FTB or gravity systems which are detached in overpressured shale rocks (Dahlen et al., 1983; Suppe, 2007; Tuitt et al., 2012; Morley et al., 2011; Yue and Suppe, 2014; Yang et al., 2016). High taper values, like those of the Chartreuse and Vercors massifs, are in the range of tectonic wedges like the Barbados accretionary prism (8°; Casey-Moore et al., 1988), the Sabah prism (10°; Hall and Wilson, 2000), the Makran accretionary prism (10°; Ellouz et al., 2007), the Hikurangi accretionary prism in New-Zealand (10°; Morley et al., 2010), or FTB like the Papua-New Guinea thrust system (12°; Hill et al., 1991), the Peruvian Sub-Andean thrust system (10°; Baby et al., 2018), or else the cordilleran system in NE Mexico (12°, Deville et

al., 2020). Such high taper tectonic wedges are associated with high pressure conditions in overpressured shale at the decollement level close to natural hydraulic fracturing conditions as shown by pressure measurements coupled with numerical modeling in the Barbados accretionary prism (Deville et al. 2010) or the Papua-New Guinea FTB (Callot et al., 2020). This interpretation is also consistent with the study of fluid inclusions in FTB like the cordilleran system in NE Mexico (Deville et al., 2020).

Indeed, in the Vercors massif, drilling results and the interpretation of seismic data show that the basal decollement is not located within halite-bearing Triassic layers, like it is the case in the Jura, but instead it is located within Lias-Dogger marly shale for which pressure measurements have shown that they were still clearly overpressured during drilling in 1959 at well SL-2 (R ratio reaching values above 1.62 at a depth of 1708 m; Table 1; Fig. 7). These high pressure values measured around the decollement level in the Vercors tectonic front, in the well SL-2, are approaching potential domains of natural hydraulic fracturing in compressive context, *i.e.* potential minimum stress values (σ_3). Indeed, this can be deduced, for instance, if we estimate the minimum stress (in MPa) *versus* depth (in m) by the following empirical relationship deduced from a worldwide study of the transition between maximum pressure and minimum leak off pressure in active tectonic areas of sedimentary basins (Grauls, 1999; Fig. 7),

$$\sigma_3 = 0.0055 (z - h)^n$$

with n between 1.17 and 1.176 in thrust fault context, between 1.156 and 1.162 in strike-fault fault context, between 1.141 and 1.147 in normal fault context. This suggests that pressure values around the decollement in the Subalpine chains are indeed close to hydraulic fracturing conditions (Fig. 7).

Also, the influence of the thickness of the series in the deformation mechanisms is illustrated if we compare the structure of the Alpine front in the Chartreuse and Vercors areas. Between these two massifs, the change of thickness in the sedimentary series is at the origin of the structural differences of the alpine front (higher propagation of the deformation front towards the foreland in the Vercors, linked to thicker series, and development of en-echelons folds; Philippe et al., 1998).

Finally, the example of the tectonic front of the western Alps illustrates how deformation of FTB is influenced by heritage prior to the compressive deformations. In particular, this example highlights how a single phenomenon (the activation of a crustal thrusting in the

ECM) can induce complex and various structures in the sedimentary cover which are largely controlled by the nature of the decollement layers and the thickness of the sediments.

6. Conclusion

This study has shown how the initial contrasts which were pre-existing before thrust tectonics at the base of the Mesozoic series have controlled the drastic differences which have developed within the FTB of the Alpine foreland during Miocene to recent late collision stages. The presence of two Triassic halite layers controlled the position of the decollement beneath the Jura (Mid-Muschelkalk and Early Keuper). Even in the areas where anhydrite-bearing sedimentary units are thick (notably the Late Keuper anhydrite-bearing unit), they have minor efficiency in terms of decollement processes and they remain poorly deformed with relatively constant thickness. The alternative activity of two halite decollement levels in the Jura favored the very large north-westward propagation of the tectonic front in the Jura area. Changes of position of the decollement from Mid-Triassic to Late Triassic halite layers linked with thrust tectonics involving former extension structures are responsible locally for tectonic subtraction during the Miocene compressive event. South of the Jura, in Chartreuse and Vercors, the interpretation of the seismic and well data has shown that the decollement is located above the Triassic formations. This is consistent with the fact that there is no massive halite in these areas (the only evaporites being thin Keuper anhydrite-bearing levels which are closely interbedded with clay-rich material). Therefore, the absence of halite is responsible for a shift of the decollement level from the Triassic in Jura to Lias-Dogger overpressured shale and marl in the Subalpine chains. The paleogeographic boundary from a halite-bearing domain to a domain with no halite had an essential influence during the Alpine deformation because it separated a northern area with a low friction decollement level from a southern area with a high basal friction decollement. Such an interpretation is consistent with the available pressure measurements. In the Jura area, fluids are not overpressured (neither in the thrust wedge nor below the decollement), whereas fluids are clearly overpressured at depth at the front of the Chartreuse and Vercors massifs (either in the immediate foreland of the FTB or within the frontal structures of the FTB). In the Jura, the low basal friction decollement is directly related to the presence of the ductile halite layers in the Triassic. Fluids are not contributing to the decollement process. Whereas, in Chartreuse and Vercors, the pressure conditions contribute to induce a decollement within Lias-Dogger shale and marls. This is also consistent with the critical taper in the different parts of the front of the Western Alps.

The thrust wedge of the Jura has a taper close to 3° which is common in salt decollement, whereas it is around 12° in Chartreuse and Vercors which is characteristic of higher friction conditions. These characteristics explain also why the Alpine foreland fold-and-thrust belt is much narrower in Chartreuse than what it is northward in the Jura where the Alpine tectonic front has propagated much more within the foreland (Fig. 2). In the southernmost part of the study area, the increasing thickness of the Mesozoic series has favored the westward propagation and the en-echelon geometry of the tectonic front of the Vercors massif. Finally, seismic data has revealed the presence of several blind thrusts which have been active during Miocene syntectonic sedimentation (Burdigalian-Langhian-Serravalian shallow marine deposits) at the tectonic front of the Chartreuse and Vercors Subalpine massifs.

Acknowledgement

I thank Alain Mascle for the several years of collaboration and exchange about the geology of the FTB of the Western Alps. He notably initiated field studies and several studies of seismic acquisition and seismic reprocessing whose results have been used in this work. I thank also Anna Sommaruga who agreed the use of the Risoux seismic line shown in her PhD Memoir. Thanks are also due to Eduard Kissling who agreed the use of geophysical data published in Lippitsch et al., 2003.

Digital Elevation Models used to complete figures 2, 3A and 5D have been downloaded at <https://pdaacsvr.cr.usgs.gov/appears/task/area>. Detailed well data are available at <https://infoterre.brgm.fr/viewer/MainTileForward.do>.

References

- Affolter, T., Gratier, J.P. (2004). Map view retrodeformation of an arcuate fold-and-thrust belt: The Jura case. *Journal of Geophysical Research* 109, B03404, <https://doi:10.1029/2002JB002270>
- Aubert, D. (1971). Le Risoux, un charriage jurassien de grandes dimensions. *Eclogae Geologicae Helvetiae*, 64, 151–156.
- Baby, P., Y. Calderón, C. Hurtado, M. Louterbach, N. Espurt, S. Brusset, M. Roddaz, S. Brichau, A. Eude, G. Calves, A. Quispe, L. Ramirez, A. Bandach, and R. Bolaños, (2018), The Peruvian Sub-Andean Foreland Basin System: Structural Overview, Geochronologic Constraints, and Unexplored Plays, in G. Zamora, K. R. McClay, and V. A. Ramos, eds., Petroleum Basins and Hydrocarbon Potential of the Andes of Peru and Bolivia. AAPG Memoir 117, <https://DOI:10.1306/13622118M1173767>
- Beck, C., Deville, É., Blanc, É., Philippe, Y., Tardy, M. (1998). Horizontal shortening control of Middle Miocene marine siliciclastic sedimentation in the southern termination of the Savoy Molasse Basin (northwestern Alps, southern Jura): combined surface and subsurface data.). in Mascle, A., Puigdefabregas, C., Luterbacher, H.P. and Fernandez, M. (eds), Cenozoic Foreland Basins of Western Europe. *Special publication of the Geological Society*, London, 134, 263-278. <https://doi.org/10.1144/GSL.SP.1998.134.01.12>
- Bellahsen, N., Mouthereau, F., Boutoux, A., Bellanger, M., Lacombe, O., Jollivet, L., Rolland, Y. (2014). Collision kinematics in the western external Alps. *Tectonics* 33 (6), 1055-1088. <https://ff10.1002/2013TC003453>
- Bergerat, F., Mugnier, J.L., Guellec, S., Truffert, C., Cazes, M., Damotte, B., Roure, F. (1990). in "Deep structure of the Alps", Roure F., Heitzmann P., Polino R. (Eds.) *Mém. Soc. Fr.* 156, *Mém. Soc. géol. suisse* 1, Vol. spec. Soc. Geol. It. 1, 145-156.
- Bonijoly, D., Perrin, J., Roure, F., Bergerat, F., Courel, L., Elmi, S., Mignot, A., and the GPF team (1996). The Ardèche palaeomargin of the South-East basin of France: Mesozoic evolution of a part of the Tethyan continental margin. *Marine and Petroleum Geology*, 13, 6, 607-623.
- Burkhard, M., Sommaruga, A. (1998). Evolution of the western Swiss Molasse basin: structural relations with the Alps and the Jura belt. *Geological Society, London, Special Publications*, 134, 279–298.
- Butler, R.W.H. (1992). Structural evolution of the western Chartreuse fold-and-thrust system, NW french subalpine chains. *Thrust tectonics*, McClay K,R, ed., Chapman and Hall, London, 287-298.
- Buxtorf, A. (1907). Zur Tektonik des Kettenjura. Bericht der Versammlung des Oberrheinischen Geologischen Veireins, 40.

Buxtorf, A. (1916). Prognosen und Befunde beim Hauensteinbasis- und Grencherberg und die Bedeutung de letzeren fur die Geologie des Jurabirges. *Verh. Naturforsh Ges. Basel* 27, 184-205.

Byerlee, J.D. (1978). Friction of rocks. *Pure and Applied Geophysics* 116, 615-626.

Callot, J.-P., Sassi, W., Roure, F., Hill, K., Wilson, N., Divies, R. (2017). Pressure and Basin Modeling in Foothill Belts: A Study of the Kutubu Area, Papua New Guinea Fold and Thrust Belt. *Petroleum Systems Analysis*, Editors: Mahdi A. AbuAlia, Isabelle Moretti, Hege M. Nordgard Bolas. *AAPG Memoir* 114, Chapter 7, 165–190, <https://DOI:10.1306/13602029M1143704>

Chapple, W.M. (1978). Mechanics of Thin-Skinned Fold-and-Thrust Belts. *Geological Society of America Bulletin* 89, 1189–1198
Carter, N. L., Hansen, F D. (1983). Creep of Rocksalt. *Tectonophysics* 92, 275-333.

Casey-Moore, J., Mascle, A. et al. (1988). Tectonics and hydrogeology of the northern Barbados Ridge: Results from Ocean Drilling Program Leg 110. *Geological Society of America Bulletin* 100(10):1578-1593. [https:// DOI:10.1130/0016-7606\(1988\)100<1578:TAHOTN>2.3.CO;2](https://DOI:10.1130/0016-7606(1988)100<1578:TAHOTN>2.3.CO;2)

Charollais, J., Davaud, E., Jamet, M. (1996). Evolution du bord oriental de la plate-forme jurassienne entre le Jurassique supérieur et l'Oligocène: modèle basé sur trois forages pétroliers (Haute-Savoie). *Géologie de la France*, 1, 25-42.

Charollais, J., Jamet, J.M. (1990). Principaux résultats géologiques du forage Brizon 1 (BZN 1), Haute-Savoie, France. *in "Deep structure of the Alps"*, Roure F., Heitzmann P., Polino R. (Eds.). *Mém. Soc. Fr.* 156, *Mém. Soc. géol. suisse* 1, *Vol. spec. Soc. Geol. It.* 1, 185-202.

Chauve, P., Martin, J., Petitjean, E., Sequeros, F. (1988). Le chevauchement du Jura sur la Bresse. Données nouvelles et interprétation des sondages. *Bull. Soc. Géol. Fr.* 8, IV, 5, 861-870.

Cobbold, P., Durand, S., Mourgues, R. (2000). Sandbox modelling of thrust wedges with fluid-assisted detachments. *Tectonophysics* 334, 245-258. <https://S0040-195140100070-1>

Dahlen, F. A. (1990). Critical taper model of fold-and-thrust belts and accretionary wedges. *Annual Review of Earth and Planetary Sciences*, 18(1), 55–99. <https://doi.org/10.1146/annurev.ea.18.050190.000415>.

Dahlen, F. A., Suppe, J. (1984). Mechanics of fold-and-thrust belts and accretionary wedges: Cohesive Coulomb theory. *Journal of Geophysical Research*, 89, 10,087–10,101. <https://doi.org/10.1029/JB089iB12p10087>

Davis, D., Suppe, J., Dahlen, F.A. (1983). Mechanics of fold-and-thrust belts and accretionary wedges. *Journal of Geophysical Research* 88 (B2), 1153-1172.

Davis, D., Engelder, T. (1985). The role of salt in fold-and-thrust belts. *Tectonophysics* 119, 67-88.

de Graciansky, P.C., Roberts, D.G., Tricart, P. (2011). The Western Alps, from Rift to Passive Margin to Orogenic Belt. In *Developments in Earth surface processes*, v. 14, 1st edition, Elsevier, 432 p. eBook ISBN: 9780444537256.

Deptuck, M.E., Kendell, K., Smith, P., 2009. Complex deepwater fold-belts in the SW Sable Subbasin, offshore Nova Scotia. *Frontiers Innovation, CSPG CSEG CWLS Convention, Calgary, Alberta Canada*. 4 pp.

Deville, E., Blanc, E., Tardy, M., Beck, C., Cousin, M., Menard, G. (1994a). Thrust propagation and syntectonic sedimentation in the Savoy Tertiary Molasse basin (Alpine foreland). *in* A. Mascle (Ed), "Hydrocarbon and Petroleum Geology of France", Pringer ed., EAPG. spec. pub. 4, 269-280. https://doi.org/10.1007/978-3-642-78849-9_19

Deville, É., Lamiroux, C., Le Bras, A., Mascle, A. (1994b). Tectonic styles and re-evaluation of petroleum plays in southeastern France. *Oil and Gas Journal*, Oct 31, 53-58.

Deville, É., Chauvière, A. (2000). Thrust tectonics in the front of the western Alps: constraints provided by the processing of seismic reflection data along the Chambéry transect. *C. R. Acad. Sci. Paris* 331, 725-732. [https://doi.org/10.1016/S1251-8050\(00\)01463-4](https://doi.org/10.1016/S1251-8050(00)01463-4)

Deville, É., Sassi, W. (2006). Contrasting thermal evolution of thrust systems: An analytical and modeling approach in the front of the Western Alps. *AAPG Bulletin*, 90, 6, 887-907. <https://DOI:10.1306/01090605046>

Deville, E., Guerlais S-H., Lallemand S., Schneider F. (2010). Fluid dynamics and subsurface sediment mobilization processes: An overview from the south-eastern Caribbean. *Basin Research, Special issue on fluid flows and Subsurface Sediment Remobilization*, v. 22, p. 361–379, <https://doi:10.1111/j.1365-2117.2010.00474x>.

Deville É. (2015). Dynamique des prismes orogéniques, le rôle des fluides. *Presses Académiques Francophones*, ISBN 978-3-8416-2683-7, 263 pages.

Deville E., Dutrannoy C., Schmitz J., Vincent B., Kohler E., Lahfid A. (2020). Shale tectonic processes: field evidence from the Parras Basin (North-Eastern Mexico). *Marine and Petroleum Geology* 122, 104688. <https://doi.org/10.1016/j.marpetgeo.2020.104688>

Doudoux, B., Mercier de Lepinay, B., Tardy, M. (1982). Une interprétation nouvelle de la structure des massifs subalpains savoyards (Alpes occidentales): nappes de charriages oligocènes et déformations superposées. *C. R. Acad. Sc. Paris*, 295, série II, 63-68.

Ellouz-Zimmermann, N., Lallemand, S., Castilla, R., Mouchot, N., Leturmy, P., Battani, A., Buret, C., Cherel, L., Desaubliaux, G., Deville, E., Ferrand, J., Legcke, A., Mahieux, G., Mascle, G., Mohr, P., Pierson-Wickmann, A.C., Robion, P., Schmitz, J., Danish, M., Hasany, S., Shahzad, A., Tabreez, A. (2007). Offshore frontal part of the Makran accretionary prism (Pakistan): the CHAMAK survey. In: *Special Volume. Thrust belts and Foreland Basins*, Chapter 18 (Ed. by O. Lacombe & F. Roure), Springer-Verlag, Berlin, 349-364.

Gidon, M. (1981). Les déformations de la couverture des Alpes occidentales externes dans la région de Grenoble, leur rapports avec le socle. *C. R. Acad. Sc., Paris*, 292, serie II, 1057-1060.

Gidon, M. (1988). L'anatomie des zones de chevauchement du massif de la Chartreuse (Chaînes subalpines septentrionale, Isère, France). *Géologie Alpine*, 64, 27-48.

Gorin, G.E., Signer, C., Amberger, G. (1993). Structural configuration of the western Swiss Molasse Basin as defined by reflection seismic data. *Eclog. Geol. Helv.* 86, 693-716.

Granado, P., Thöny, W., Carrera, N., Gratzer, O., Strauss, P., Munoz, J.A. (2016). Basement-involved reactivation in fold and thrust belts: the Alpine-Carpathian Junction (Austria). *Geological magazine*, 153(5-6), 1100-1135.

Grauls, D. (1999). Overpressure: causal mechanism, conventional and hydromechanical approaches. *Oil & Gas Sci. & Technol.*, 54, 667-678. <https://doi.org/10.2516/ogst:1999056>

Guellec, S., Mugnier, J.-L., Tardy, M., Roure, F. (1990a). Neogene evolution of the western Alpine foreland in the light of ECORS data and balanced cross-section. in "Deep structure of the Alps", Roure F., Heitzmann P., Polino R. (Eds.) *Mém. Soc. Fr.* 156, *Mém. Soc. géol. suisse* 1, Vol. spec. *Soc. Geol. It.* 1, 165-184.

Guellec, S., Lajat, D., Mascle, A., Roure, F., Tardy, M. (1990b). Deep seismic profiling and petroleum potential in the western Alps: constraints with ECORS data, balanced cross-sections and hydrocarbon modeling, in B. Pinet and C. Bois (Eds.) "The Potential of Deep Seismic Profiling for Hydrocarbon Exploration", Ed. Technip, Paris, 425-438.

Hall, R., Wilson, M.E.J. (2000). Neogene sutures in eastern Indonesia. *J. Asian Earth Sci.* 18, 781-808.

Hill, K.C. (1991). Structure of the Papuan Fold Belt, Papua New Guinea. *American Association of Petroleum Geologists Bulletin* 75, 857-872.

Hubbert, M.K., Rubey, W.W. (1959). Role of fluid pressure in mechanics of overthrust faulting: I. Mechanics of fluid-filled porous solids and its application to overthrust faulting. *Geological Society of America Bulletin*, 70, 115-66.

Hudec, M.R., Jackson, M.P.A., 2004. Regional restoration across the Kwanza Basin, Angola: salt tectonics triggered by repeated uplift of a metastable passive margin. *AAPG Bulletin* 88, 971-990.

Hua, Y., Zhao, D., Xu, Y. (2017). P wave anisotropic tomography of the Alps. *J. Geophys. Res. Solid Earth*, 122, 4509-4528. <https://doi:10.1002/2016JB013831>

Jordan, P. (1992). Evidence for large-scale decoupling in the evaporites of Northern Switzerland: an overview. *Eclog. Geol. Helv.* 85, 3, 677-693.

- Jordan, P., Noack, T., Widmer, T. (1990). The evaporite shear zone of Jura boundary thrust – New evidence from Wiesen well (Switzerland). *Eclogae Geologicae Helveticae*, 83, 525–542.
- Jordan, P., Nüesch, R. (1989a). Deformation structures in the Muschelkalk anhydrites of the Schafisheim Well (Jura Overthrust, Northern Switzerland). *Eclogae Geologicae Helveticae*, 82(2), 429–454.
- Jordan, P., & Nüesch, R. (1989b). Deformational behavior of shale interlayers in evaporite detachment horizons, Jura overthrust, Switzerland. *Journal of Structural Geology*, 11(7), 859–871.
- King-Hubbert, M., 1951. Mechanical basis for certain familiar geological structures. *Bulletin of the Geological Society of America* 62, 355-372.
- Laubscher, H. P. (1961). Die Fernschubhypothese der Jurafaltung. *Eclogae geol. Helv.* 54, 221-282
- Laubscher, H.P. (1972). Some overall aspects of Jura dynamics. *Am. J. Sci.* 272, 293-318.
- Laubscher, H.P. (1981). The 3D propagation of decollement in Jura. In McClay K.R. and Price N.J. (ed): Thrust and nappe tectonics. *Geol. Soc. Spec. publ.*,9, 311-318. <https://doi.org/10.1144/GSL.SP.1981.009.01.27>
- Lippitsch R., E. Kissling, J. Ansorge (2003). Upper mantle structure beneath the Alpine orogen from high-resolution teleseismic tomography. *Journal of Geophysical Research*, 108, B8, 2376.
- Madritsch, H., Schmid, S.M., Fabbri, O. (2008). Interactions between thin- and thick-skinned tectonics at the northwestern front of the Jura fold-and-thrust belt (Eastern France). *Tectonics*, 27(5), <http://dx.doi.org/10.1029/2008tc002282>.
- Looser, N., H. Madritsch, M. Guillong, O. Laurent, S. Wohlwend, S. M. Bernasconi (2021). Absolute age and temperature constraints on deformation along the basal décollement of the Jura Fold-and-thrust Belt from carbonate U-Pb dating and Clumped Isotopes. *Tectonics* <https://doi:10.1029/2020TC006439>
- Malz, A., Madritsch, H., Jordan, P., Meier, B., Kley, J. (2019). [Along-strike variations in thin-skinned thrusting style controlled by pre-existing basement structure in the easternmost Jura Mountains \(Northern Switzerland\)](https://doi.org/10.1144/SP490-2019-090). Geological Society, London, Special Publications, 490, 199-220, <https://doi.org/10.1144/SP490-2019-090>
- Masclé, A., Vially, R., Deville, É., Biju-Duval, B., Roy, J.P. (1996). The petroleum evaluation of a tectonically complex area: the western margin of the southeast basin (France). *Marine and Petroleum Geology*, 13, 8, 941-961. [https://doi.org/10.1016/S0264-8172\(96\)00041-4](https://doi.org/10.1016/S0264-8172(96)00041-4)
- Menard, G., Thouvenot, F. (1986). Coupes équilibrées crustales : méthodologie et application aux Alpes occidentales. *Rev. Geol. Dyn. Géogr. Phys.*, 1, 35-44.
- Michel, P., Appert, G., Lavigne, J., Lefavrais, A., Bonte, A., Lienhardt, G., Ricour, J. (1953). Le contact Jura-Bresse dans la région de Lons-le-Saunier. *Bull. Soc. géol. Fr.* 3, 593-611.

- Mock, S., von Hagke, C., Schlunegger, F., Dunkl, I., Herwegh, M. (2020). Long-wavelength late-Miocene thrusting in the north Alpine foreland: implications for late orogenic processes. *Solid Earth*, 11, 1823–1847, <https://doi.org/10.5194/se-11-1823-2020>
- Morley, C.K., King, R., Hillis, R., Tingay, M., Backe, G. (2011). Deepwater fold and thrust belt classification, tectonics, structure and hydrocarbon prospectivity: A review. *Earth Science review* 104, 41-91. <https://doi.org/10.1016/j.earscirev.2010.09.010>
- Mugnier, J.L., Viallon, P. (1986). Deformation and displacement of the Jura cover on its basement. *J. Struc. Geol.*, 8, 373-387.
- Mugnier, J.L., Guellec, S., Menard, G., Roure, F., Tardy, M., Vialon, P. (1990). A crustal scale balanced cross-section through the external Alps deduced from the ECORS profile. in "Deep structure of the Alps", Roure F., Heitzmann P., Polino R. (Eds.) *Mém. Soc. Fr.* 156, *Mém. Soc. géol. suisse* 1, Vol. spec. Soc. Geol. It. 1, 203-216.
- Peel, E.J., Hossack, J.R., Travis, C.J. (1995). Genetic structural provinces and salt tectonics of the Cenozoic offshore U.S. Gulf of Mexico: a preliminary analysis. In: Jackson, M.P.A., Roberts, D.G., Snelson, S. (Eds.), *Salt Tectonics: A Global Perspective: AAPG Mem.*, 65, 153–175.
- Pfiffner, O.A., Lehner, P., Heitzmann, P., Muller, S., Steck, A. (1997). *Deep structure of the Swiss Alps, results of NRP20*. Chapter 8, 64-72. Birkhauser Verlag Basel 448 p.
- Philippe, Y., Colletta, B., Deville, É., Mascle, A. (1996). The Jura fold-and-thrust belt: a kinematic model based on map-balancing. in Ziegler, P.A. and Horvath, F. (Eds), *Peri-Tethys Memoir 2: Structure and prospects of Alpine Basins and Forelands. Mém. Mus. natn. Hist. nat.*, 170, 235-261.
- Philippe, Y., Deville, É., Mascle, A. (1998). Thin-skin inversion tectonics at oblique basin margins: example of the western Vercors and Chartreuse Subalpine massifs (southeastern France). in Mascle, A., Puigdefabregas, C., Luterbacher, H.P. And Fernandez, M. (eds), *Cenozoic Foreland Basins of Western Europe. Special publication of the Geological Society*, London, 134, 239-262. <https://doi.org/10.1144/GSL.SP.1998.134.01.11>
- Rime, V., Sommaruga, A., Schori, M., Mosar, J. (2019). Tectonics of the Neuchatel Jura Mountains: insights from mapping and forward modeling. *Swiss Journal of Geosciences*, 112, 563–57. <https://doi.org/10.1007/s00015-019-00349-y>
- Rigassi, D. (1977). Encore le Risoux. *Bull. Soc. Vaud. Sc. Nat.*, no 352, vol.73.
- Ross, J.V., Bauer, S.J. (1992). Semi-brittle deformation of anhydrite-halite shear zones simulating mylonite formation. *Tectonophysics*, 213, 303-320.
- Sanchis, E., Seranne, M. (2000). Structural style and tectonic evolution of a polyphase extensional basin of the Gulf of Lion passive margin : the Tertiary Alès Basin, southern France. *Tectonophysics*, 322, 243-264.

- Sommaruga, A. (1997). Geology of the Central Jura and the Molasse basin: New insight into an evaporite-based foreland fold and thrust belt. *Mémoires de la Société Neuchateloise de Sciences Naturelles*, 12, pp. 176.
- Sommaruga, A. (1999). Decollement tectonics in the Jura foreland fold-and-thrust belt. *Marine and Petroleum Geology*, 16, 111–134.
- Sommaruga, A. (2011). From the central Jura Mountains to the Molasse Basin (France and Switzerland). *Swiss Bulletin fur angewandte Geologie*, 16, 63–75.
- Sommaruga, A., Eichenberger, U., Marillier, F. (2012). Seismic Atlas of the Molasse Basin. Swiss Geological Survey: Federal Office of Topography swisstopo.
- Sommaruga, A., Mosar, J., Schori, M., and Gruber, M. (2017). The role of the Triassic evaporites underneath the North Alpine foreland. In Soto, J., Flinch, J., and Tari, G., (Ed.), Permo-Triassic salt provinces of Europe, North Africa and the Atlantic Margins: tectonics and hydrocarbon potential, chapter 22 (IV). Elsevier.
- Suppe, J. (2007). Absolute fault and crustal strength from wedge tapers. *Geology*, 35, 1127–1130. <https://doi:10.1130/G24053A.1>.
- Tardy, M., Deville, E., Fudral, S., Guellec, S., Ménard, G., Thouvenot, F., Vialon, P. (1990). Interprétation structurale des données de sismique réflexion profonde ECORS-CROP Alpes entre le front pennique et la ligne du Canavese (Alpes occidentales), in "Deep structure of the Alps", Roure F., Heitzmann p., Polino R. (Eds.) *Mém. Soc. Fr.* 156, *Mém. Soc. géol. suisse* 1, Vol. spec. *Soc. Geol. It.* 1, 217-226.
- Thouvenot, F., Paul, A., Senechal, G., Hirn, A., Nicolich, R. (1990). ECORS-CROP wide-angle reflection seismics: Constraints on deep interfaces beneath the Alps. in "Deep structure of the Alps", Roure F., Heitzmann p., Polino R. (Eds.) *Mém. Soc. Fr.* 156, *Mém. Soc. géol. suisse* 1, Vol. spec. *Soc. Geol. It.* 1, 97-106.
- Thouvenot, F., Ménard, G. (1990). Allochthony of the Chartreuse Subalpine massif: explosion-seismology constraints. *J. Struct. Geol.*, 2, 1, 113-121. [https://doi.org/10.1016/0191-8141\(90\)90052-Z](https://doi.org/10.1016/0191-8141(90)90052-Z)
- Trudgill, B.D., Rowan, M.G., Fiduk, J.C., Weimer, P., Gale, P.E., Korn, B.E., Phair, R.L., Gafford, W.T., Roberts, G.E., Dobbs, S.W. (1999). The Perdido Fold Belt, Northwestern Deep Gulf of Mexico. Part 1: Structural Geometry, Geolution and Regional Implications: AAPG Bulletin, 83, 88–113.

Tuitt, A., King, R., Hergert, T., Tingay, M., Hillis, R. (2012). Modelling of sediment wedge movement along low-angle detachments using ABAQUS™. *Geological Society, London, Special Publications*, 367, 171-183. <https://doi.org/10.1144/SP367.12>

Vergés, J., E. Saura, E. Casciello, M. Fernández, A. Villaseñor, I. Jiménez-Munt & D. García-Castellanos (2011). Crustal-scale cross-sections across the NW Zagros belt: implications for the Arabian margin reconstruction. *Geol. Mag.* 148 (5–6), 739–761.

von Hagke, C., Cederbom, C.E., Oncken, O.,1 Stöckli, D.F., Rahn, M.K., Schlunegger, F. (2012). Linking the northern Alps with their foreland: The latest exhumation history resolved by low-temperature thermochronology. *Tectonics*, 31, TC5010, <https://doi:10.1029/2011TC003078>

von Hagke, C., Oncken, O., & Evseev, S. (2014). Critical taper analysis reveals lithological control of variations in detachment strength; an analysis of the Alpine basal detachment (Swiss Alps). *Geochemistry, Geophysics and Geosystems*, 15(1), 176–191.

Wildi, W., Huggenberger, P. (1993). Reconstitution de la plateforme européenne anté-orogénique de la Bresse aux Chaines Subalpines; éléments de cinématique alpine (France et Suisse occidentale). *Eclogae Geologicae Helvetiae*, 86, 47–64.

Winnock, F. (1961). Résultats géologiques du forage Risoux 1. *Bull. Ver. Scheiz. Petrol. Geol. U-ing*, 28, 74, 17-26.

Yang, C-M., J.-J. Dong, Y.-L. Hsieh, H.-H. Liu, C.-L. Liu (2016). Non-linear critical taper model and determination of accretionary wedge strength. *Tectonophysics* 692 (2016) 213–226. <http://dx.doi.org/10.1016/j.tecto.2016.04.026>

Yue, L.-F., Suppe, J. (2014). Regional pore-fluid pressures in the active western Taiwan thrust belt: A test of the classic Hubbert-Rubey fault-weakening hypothesis. *Journal of Structural Geology* 69, 493-518.

Ziegler, P.A. (1994). Cenozoic rift system of Western and Central Europe: An overview. *Geol. Mijnbow* 73, 99-127.

FIGURES CAPTION

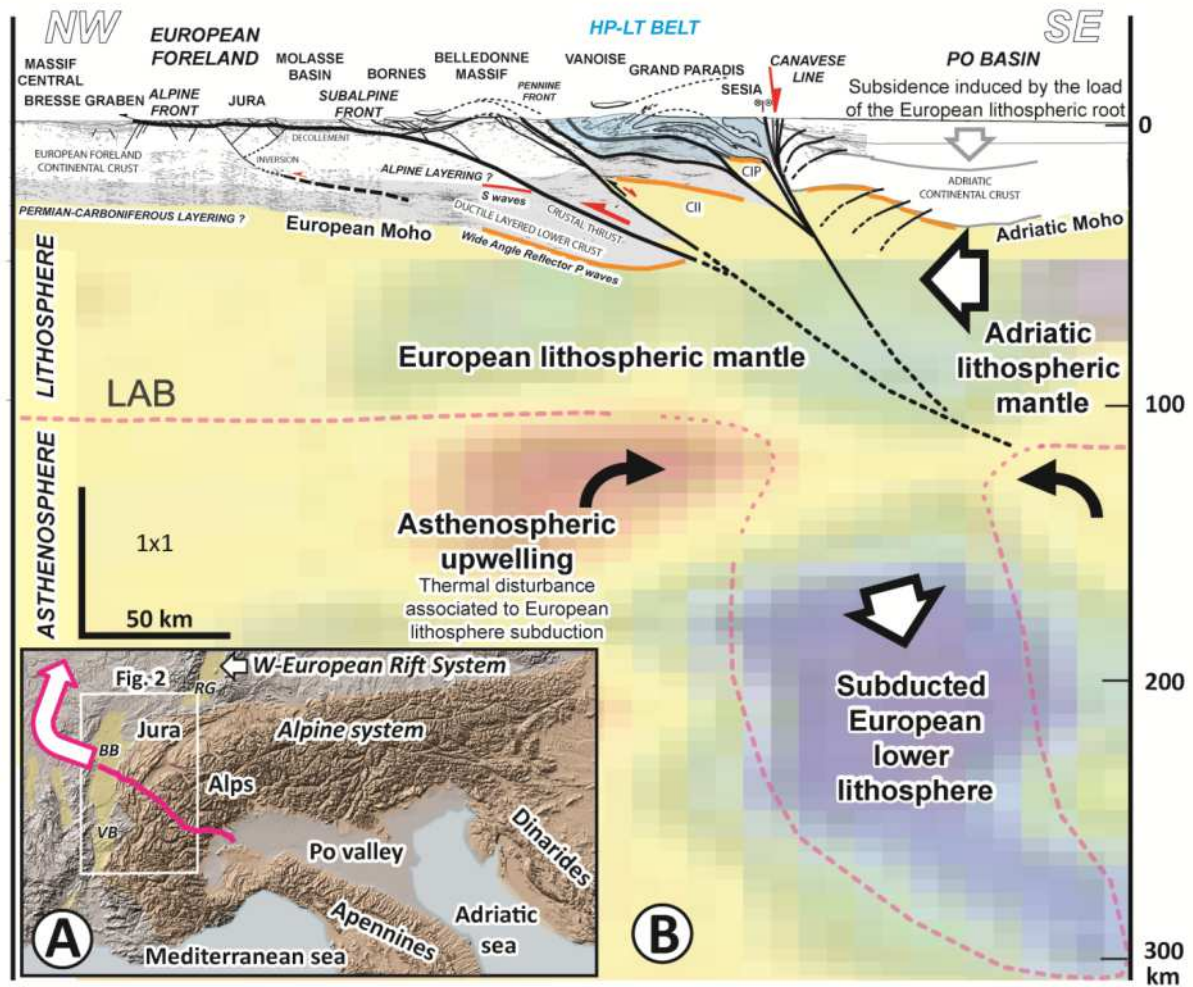


Figure 1. **A.** Location of the study area and location of the lithospheric transect along the ECORS-CROP deep seismic profile presented in Fig. 1B (RG: Rhine graben, BB: Bresse Basin; VB: Valence Basin). **B.** Large scale structure of the Western Alps based on the compilation of studies of vertical and wide angle seismic reflection, and on tomographic study of the P-Waves velocity. Line drawing modified from Deville (2015). Structural interpretation modified from the interpretation Deville, Fudral, Thouvennot, Tardy published in Tardy et al. (1990). Wide angle reflection P-waves data are from Thouvennot et al. (1990). The mantle structure is deduced from a tomographic study of the P-waves velocity from Lippitsch et al. (2003) (projection along the ECORS-CROP profile). LAB: lithosphere-asthenosphere boundary. CII: lower Ivrea mantle body, CIP: Main Ivrea mantle body.

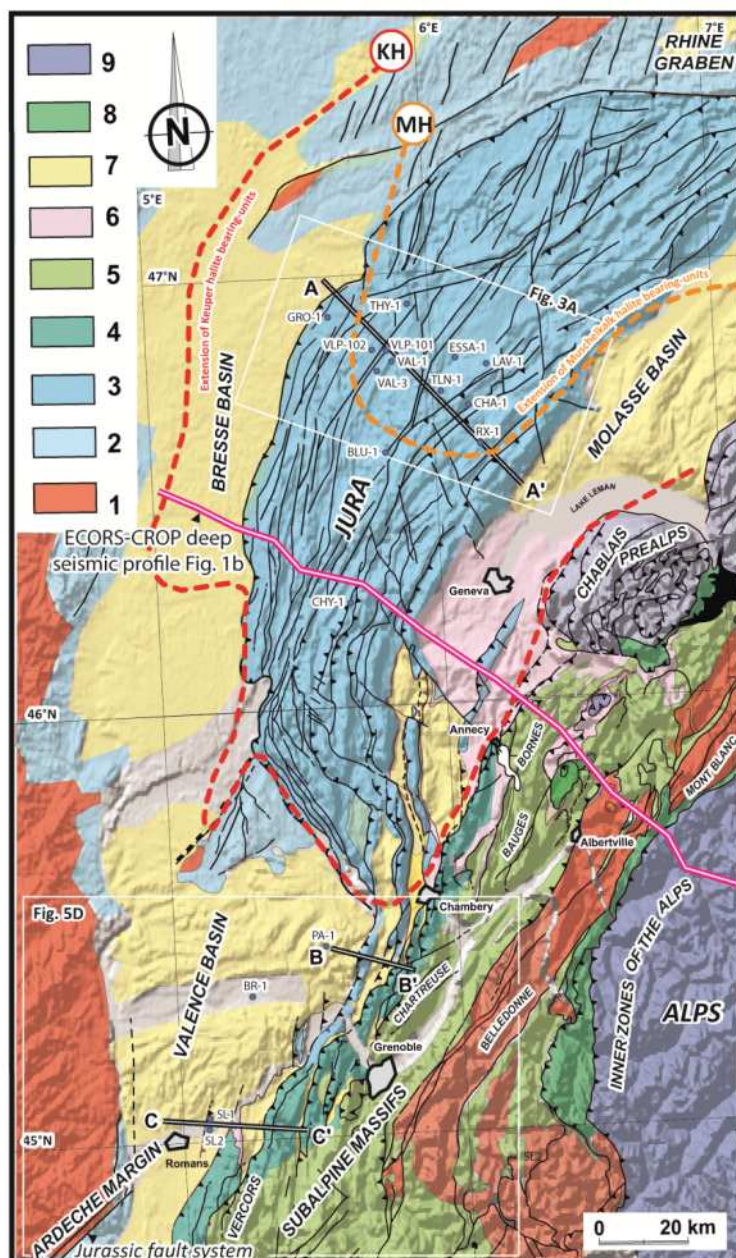


Figure 2. Structural sketch-map of the western Alps tectonic front (with location of the wells with pressure measurements shown in Table 1 and location of the cross-section shown in Fig. 8). - 1. Crystalline basement; 2. Autochthonous Mesozoic cover; 3. Allochthonous Mesozoic cover of platform facies; 4. Allochthonous Pre-Subalpine Mesozoic cover; 5. Allochthonous Subalpine Mesozoic cover; 6. Eocene-Aquitainian; 7. Miocene-Pliocene; 8. Ultra-Dauphinois zone; 9. Inner zones of the Alps. MH orange dotted line: Extension of the Muschelkalk (Mid-Triassic) halite-bearing unit. KH red dotted line: Extension of the Keuper (Late Triassic) halite-bearing unit. A-A', B-B' and C-C' correspond to the location of the cross-sections of Fig. 8A.

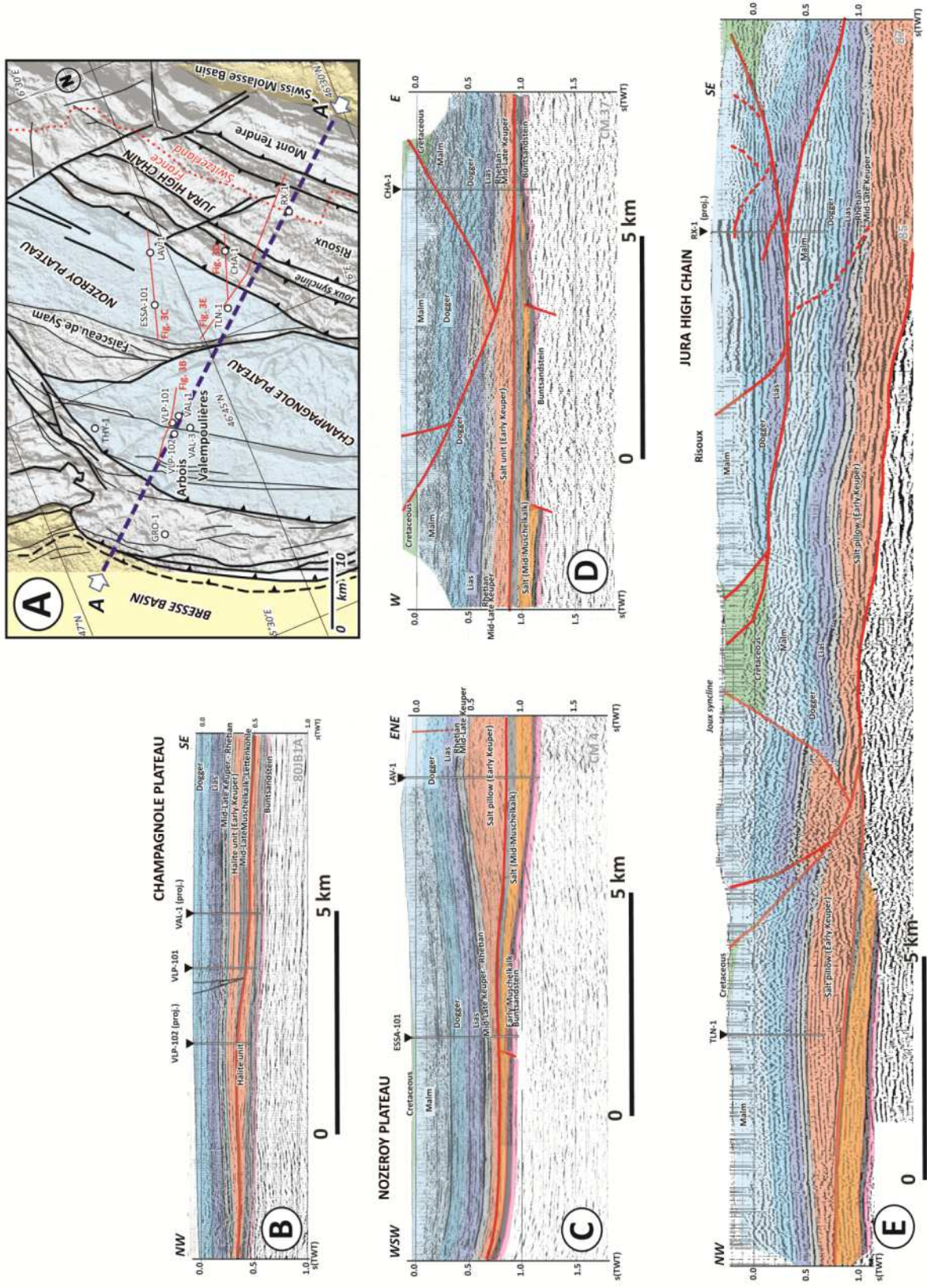


Figure 3. Seismic profiles in central Jura.

A. Structural sketch-map with location of the seismic lines (A-A': location of the Jura cross-section presented in Fig. 8).

B. Seismic line illustrating the duplication of the Mid-Triassic in the Valempoulières area.

C. Seismic line illustrating the subtraction of the Mid-Triassic in the Essavilly area.

D. Seismic line illustrating the pop-up structure of the Chatelblanc area.

E. Seismic composite line illustrating the duplication of the Mesozoic series in the eastern high chain of the Jura.

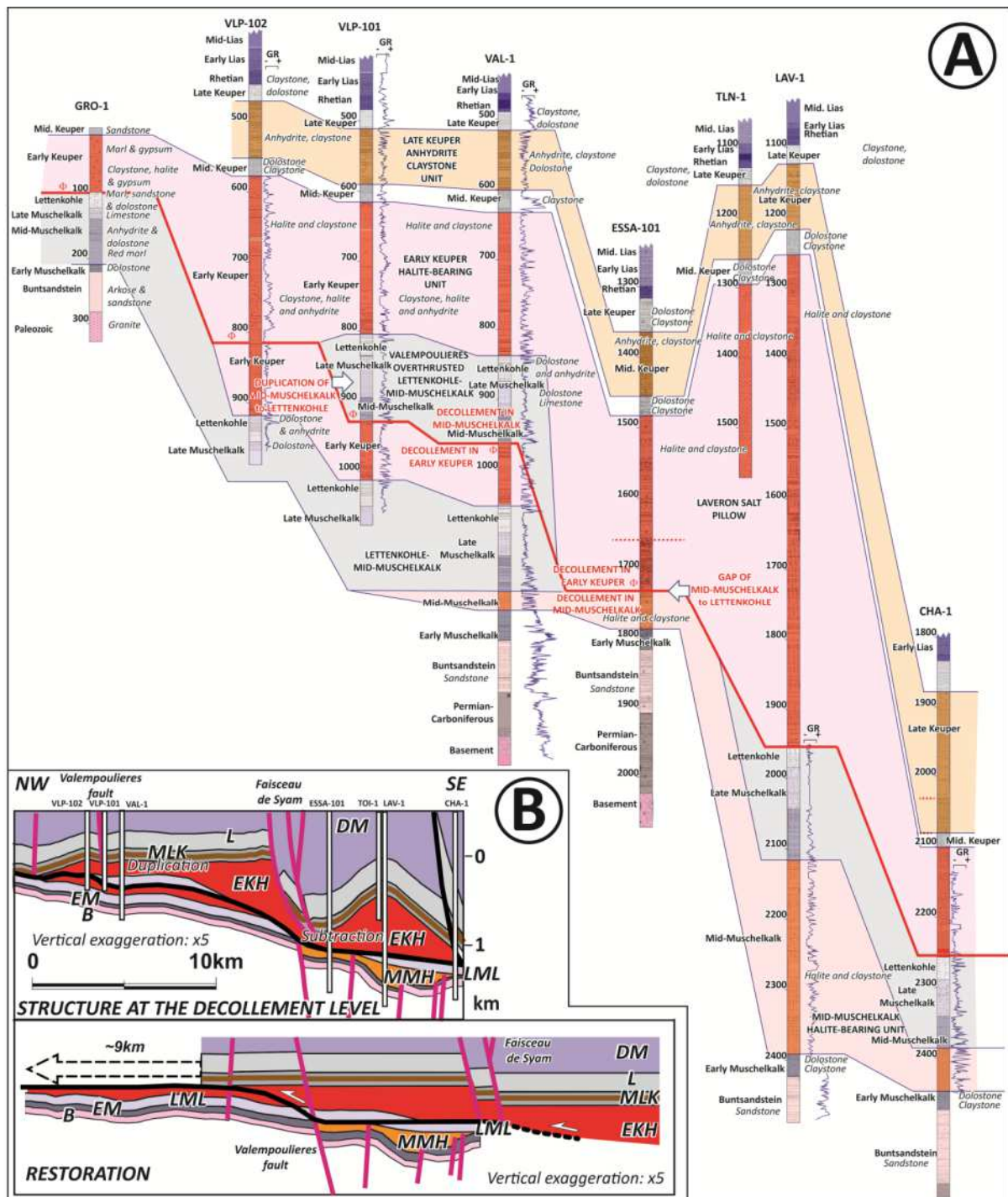


Figure 4. A. Correlation of stratigraphic logs at the base of the Mesozoic series, focusing from Mid-Lias to the Basement when reached. This illustrates the position of the decollement level in central Jura from the available public final drilling reports. Gamma ray measurements are shown when available (depths below surface; detailed well data available at www.infoterre.brgm.fr). **B.** Structural cross-section at the decollement level, B: Buntsandstein, EM: Early Muschelkalk, MMH: Mid-Muschelkalk halite-bearing unit, LML:

Late-Muschelkalk-Lettenkohle, EKH: Early Keuper halite-bearing unit, MLK: Mid- to Late Keuper including Late Keuper anhydrite-bearing unit in brown, L: Lias, DM: Dogger-Malm.

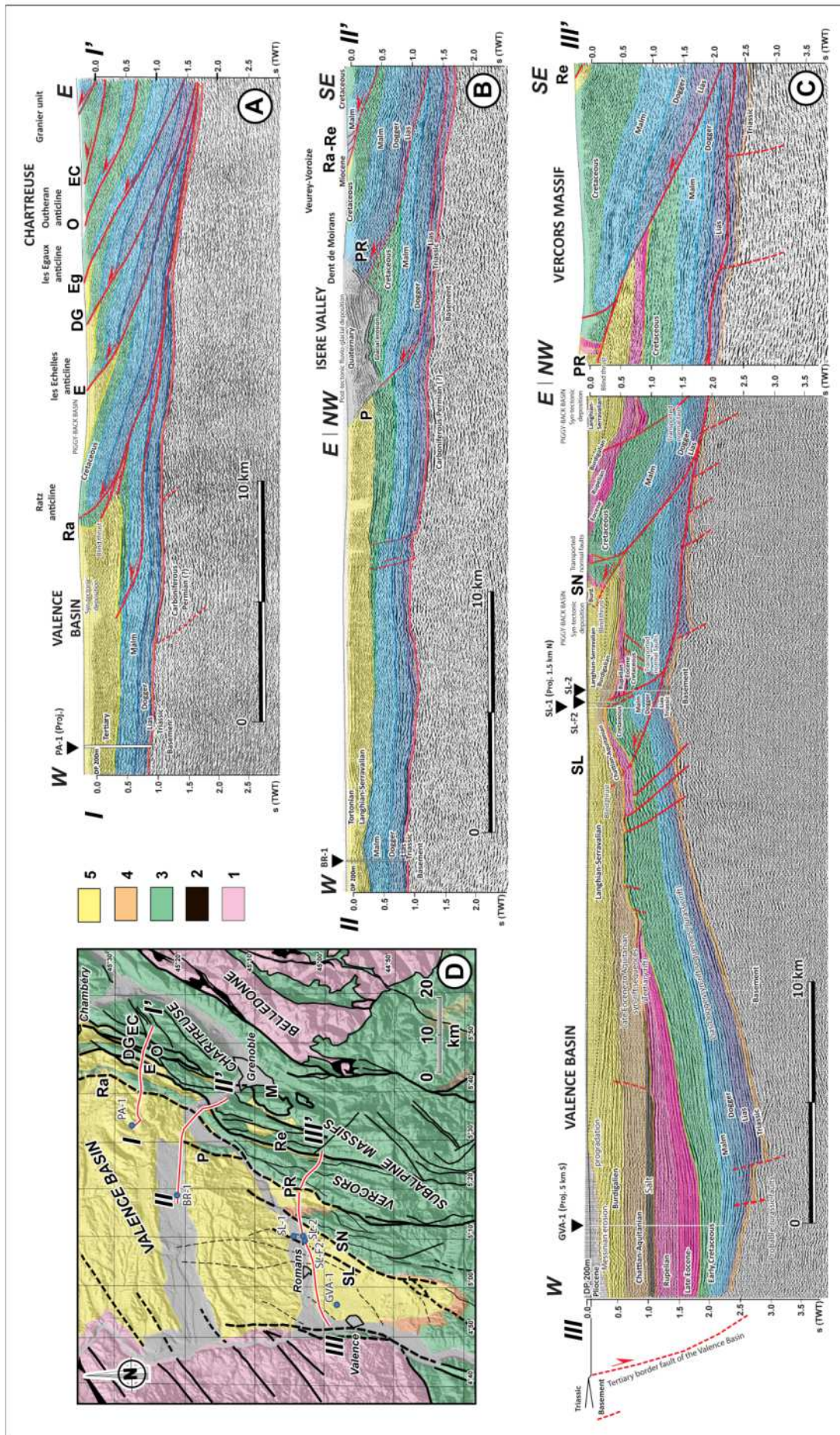


Figure 5. Seismic profiles acquired at the front of the Chartreuse and Vercors massifs.

- A.** Seismic line in the front of the Chartreuse massif.
- B.** Seismic line at the northern edge of the Vercors massif.
- C.** Seismic line in the Valence basin and the front of the Vercors massif.
- D.** Structural sketch and location of the seismic lines.

Note the spectacular stack of tectonic units in the Chartreuse massif. Note also the important Quaternary infill to the north-west of the Vercors, consequence of a strong glacial overcrowding.

1: Pre-Triassic basement; 2. Carboniferous-Permian basins; 3. Mesozoic series ; 4. Eocene-Aquitania syn-rift series ; 5. Miocene-Pliocene series.

Ra: Ratz thrust; E: Les Echelles thrust; DG: Entre-deux-Guiers thrust; Eg : Les Egaux thrust; O : Outheran thrust ; EC : Eastern Chartreuse thrust; SL: Saint-Lattier thrust; SN: Saint-Nazaire thrust; PR: Pont-en-Royans thrust; P: Polienas thrust; R: Rencurel thrust; R: Rencurelthrust; M: Moucherotte thrust.

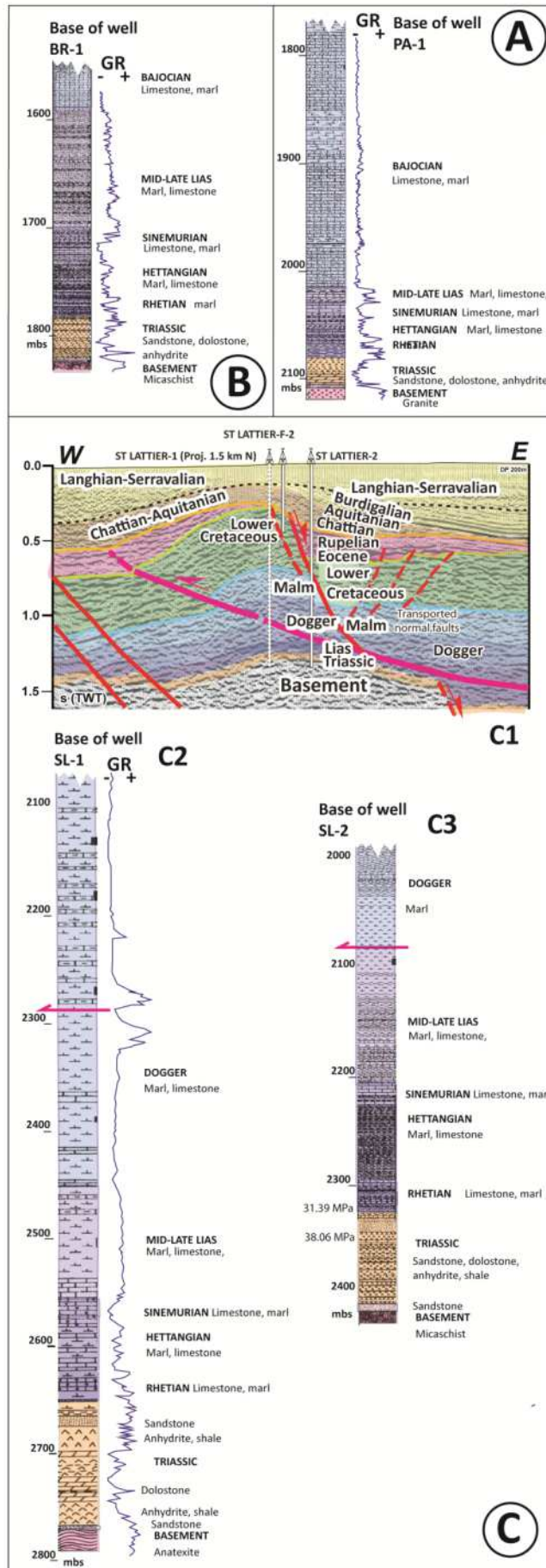


Figure 6. Information about the base of the Mesozoic series provided by wells drilled in the Valence Basin. **A.** Base of well PA-1. **B.** Base of well BR-1. **C.** Subsurface data in the area of Saint-Lattier. C1: seismic profile of the Saint-Lattier area; C2: Base of the well SL-1; C3: Base of the well SL-2 (detailed well data available at www.infoterre.brgm.fr).

Figure 7. A. Pressure measurements *versus* depth below surface within the Jura Mountains, Valence basin and Vercors thrust front. Global trends of minimum stress deduced from the transition between maximum pressure measurements and minimum leak off pressure in active tectonic areas are represented for normal fault context (yellow), strike-slip fault context (orange) and thrust fault context (pink), worldwide compilation from Grauls (1999). Fluids are underpressured in the Jura Mountains, whereas they reach elevated overpressure in the Subalpine front in the condition of thrusting and decollement tectonics. **B.** Pressure measurements *versus* mean sea level within the Jura Mountains. The reservoirs located below the Jura decollement are regarded as being in hydrostatic condition (water column density 1.07 g/cm^3) with an equilibrium level with atmosphere at 250 m of elevation ($R^2= 0.995$). Reverse pressure gradient is seen in the inner Jura between the fluids located above and below the decollement. **C.** Pressure measurements *versus* mean sea level within the Valence basin and Subalpine thrust front (Vercors).

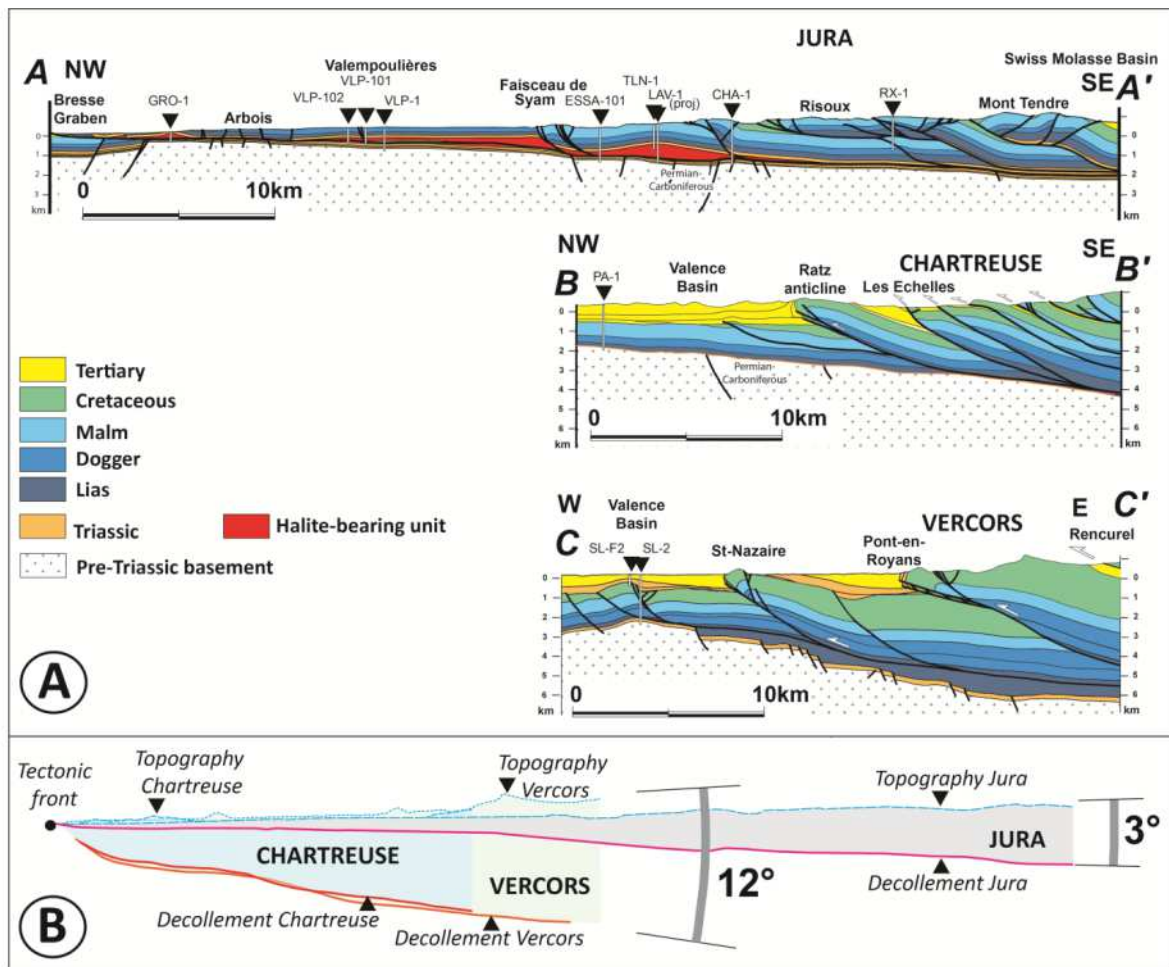


Figure 8. A. Comparison of the structure of the Alpine front between the Jura Mountains, the Chartreuse massif and the Vercors massif (sections based on the interpretation of available seismic data; location of the sections in Fig. 2). Note that the Triassic along the Chartreuse section is very thin at the scale of the section (included within the orange line). The low angle wedge of the Jura Mountains is due to halite-bearing units at the basal decollement level (cross-section modified from Deville, 2015). The high angle wedges of the Chartreuse and Vercors massifs is linked to the absence of halite and a less efficient decollement level associated with high pressure conditions (Cross-sections modified from Deville and Sassi, 2006). Note that the locations these straight cross-sections are not fitting exactly the locations of seismic lines shown in 3 and 5. **B.** Comparison of the tapers between the Jura, Chartreuse and Vercors massifs.

Well acronym	Longitude (°E)	Latitude (°N)	Elevation (m)	Formation age	Depth below surface (r)	Depth bsl (m)	Pressure (MPa)
JURA							
THY-1	5.32173913	46.90767697	702.8	Lettenkohle	520	-182.8	1.66
				Mid-Muschelkalk	650.1	-52.7	3.02
				Buntsandstein	1002.7	293.9	5.86
BD-101	5.617535	46.6647911	535	Lettenkohle	680	145	4.61
BD-105	5.6148421	46.6645983	542	Lettenkohle	694	152	6.08
ET-1	6.0094913	47.0074686	524	Buntsandstein	1230	706	10.1
VAL-1	5.8752561	46.817491	653	Lettenkohle (upper unit)	867	214	6.38
				Lettenkohle (lower unit)	1032	439	8.31
				Buntsandstein	1253	600	9.43
VAL-3	5.8519241	46.8085202	633	Lettenkohle (upper unit)	868	235	6.47
				Lettenkohle (lower unit)	1045	412	6.52
ESSA-101	6.078337185	46.78648488	790	Hettangian	1324.5	534.5	12.62
				Early Muschelkalk	1811.5	1021.5	13.11
CHA-1	6.10703218	46.67872072	1021.6	Late Muschelkalk	2249	1227.4	17.59
				Late Muschelkalk	2290	1268.4	18.12
				Late Muschelkalk	2340	1318.4	18.72
				Late Muschelkalk	2349	1327.4	18.58
				Early Muschelkalk	2442	1420.4	16.9
				Buntsandstein	2450	1428.4	17.68
BLU-1	5.86154974	46.59047377	803.26	Late Muschelkalk	1642	838.7	12.1
				Late Muschelkalk	1645.5	842.2	12.19
				Early Muschelkalk	1679	875.7	12.83
				Buntsandstein	1791.5	988.2	13.34
				Buntsandstein	1795.5	992.2	13.43
				Buntsandstein	1807.8	1004.5	13.53
				Buntsandstein	1811.5	1008.2	13.62
				Buntsandstein	1822.5	1019.2	13.73
				Buntsandstein	1316	505.2	7.82
Buntsandstein	1327	516.16	7.91				
Basement	1351	540.16	7.84				
VALENCE BASIN - SUBALPINE CHAINS							
PA-1	5.54105476	45.4493155	543	Triassic	2087.5	1544.5	21.29
				Basement	2115.5	1576.5	21.29
BR-1	5.31157248	45.34663088	365	Late Lias	1605	1240	15.5
				Triassic	1809	1444	20.31
				Top basement	1825	1460	20.6
SL-1	5.19427626	45.08733906	183.7	Oligocene	468	284.3	3.43
				Malm	1201	1017.3	11.77
SL-2	5.17183343	45.04842731	202	Malm	1186	984	11.01
				Dogger	1707	1505	27.76
				Dogger	1708	1506	28.06
				Rhetian	2319	2117	31.39
				Triassic	2350	2148	38.06

Table 1. Pressure measurements